STATE OF KNOWLEDGE OF THE PLUTO-CHARON SYSTEM

TAKEN FROM THE REPORT OF THE PLUTO SCIENCE DEFINITION TEAM

June 1999

STATE OF KNOWLEDGE OF THE PLUTO-CHARON SYSTEM

TABLE OF CONTENTS

TABLE OF TABLES

TABLE OF FIGURES

STATE OF KNOWLEDGE OF THE PLUTO-CHARON SYSTEM

TAKEN FROM THE REPORT OF THE PLUTO SCIENCE DEFINITION TEAM

Since the Outer Planets AO is asking for proposals that describe a complete Pluto remote sensing or radio science investigation, the scope of this report describing the state of knowledge of the Pluto-Charon system and the outstanding scientific questions is quite comprehensive. The report is drawn essentially verbatim from the Pluto Science Definition Team (SDT) report* to NASA, which can be found in its entirety on the World Wide Web, http://www.lpl.arizona.edu/pluto. Since the issuing of that report, the reference trajectory and spacecraft configuration have undergone significant changes to reflect changes in the launch date and advances in spacecraft capability. In the event of conflict between the Science Definition Team Report description of the Pluto Express mission and this AO, the AO takes precedence. The basic parameters of the reference mission and the Pluto "strawman payload" were developed by the Outer Planets Science Working Group** prior to the formation of the Pluto Science Definition Team.

1. Introduction

Fifteen years ago we did not know enough about Pluto and Charon to merit a substantial review article in a refereed journal. Today, the situation is different, with the recent publication of a major book on these objects (Stern and Tholen, 1997) and substantial commitment of ground-based and orbital facilities for continuing observations. The following summary of our knowledge is intended to give a flavor for the intellectual foundation around which a first reconnaissance mission is being designed. It must be emphasized that in each of the disciplines covered, *significant questions exist which can be addressed best (or only) by a close flyby mission.* Table 1 summarizes the basic parameters of the Pluto-Charon system.

2. Orbital Parameters

Pluto and Charon lie at a mean distance from the Sun of 39.4 AU; their heliocentric orbit was determined with reasonable accuracy within the first few years following Pluto's discovery in 1930. However, with prediscovery observations extending back only as far as 1915, observations presently span only about one-third of the 248-year orbital period. As a result, the mean motion is still not known as well as for the other planets, which limits the accuracy with which long-term numerical integration's can be performed. The integration's that have been done show Pluto to be in a 2:3 resonance with Neptune, which prevents close approaches to that planet. The resonance has not been seen to break over the length of the integrations, which now extend to the age of the solar system.

[*] *Pluto-Kuiper Express Science Definition Team Report*, J. Lunine, ed., October 1995. The membership of the Pluto Express Science Definition Team as of October 1995 is as follows:	[**] The membership of the Outer Planets Science Working Group as of October 1995 is as follows:
Jonathan I. Lunine (Chair), The University of Arizona Dale Cruikshank, NASA Ames Research Center Academician Albert A Galeev, Space Research Institute (IKI) Don Jennings, NASA Goddard Space Flight Center David Jewitt, University of Hawaii Slava Linkin, Space Research Institute (IKI) Ralph McNutt, APL Johns Hopkins University Fritz Neubauer, Universitaet Koeln Laurence Soderblom, USGS Branch of Astrogeology Alan Stern, Southwest Research Institute (Boulder) Richard Terrile, JPL David Tholen, University of Hawaii Len Tyler, Stanford University Roger Yelle, Boston University	Alan Stern (Chair), Southwest Research Institute (Boulder) Fran Bagenal, University of Colorado Robert H. Brown, University of Arizona Mark Buie, Lowell Observatory Andrew Cheng, Applied Physics Laboratory Thomas Cravens, University of Kansas Dale Cruikshank, NASA Ames Research Center James Elliot, Massachusetts Institute of Technology Michael Flasar, Goddard Space Flight Center William Hubbard, University of Arizona Andrew Ingersoll, California Institute of Technology Torrence Johnson, JPL Jonathon Lunine, University of Arizona Esam Marouf, San Jose State University William McKinnon, Washington University Duane Muhleman, California Institute of Technology Toby Owen, University of Hawaii Larry Soderblom, USGS Flagstaff Richard Terrile, JPL David Tholen, University of Hawaii Larry Trafton, University of Texas Leonard Tyler, Stanford University Roger Yelle, Boston University David Young, Southwest Research Institute Richard Young, NASA Ames Research Center

Table 1: Basic parameters of Pluto System

Parameter	**Pluto**	**Charon**
Rotation Period	6.3872 days	6.3872 days
Radius	1164-1187	590-630 km
Perihelion V_o	13.6 mag	15.5 mag
B Geometric Albedo	0.55	0.32
V-I Color	0.93 mag	0.83 mag
Known Surface Ices	CH_4, N_2, CO	H_20
Atmosphere	Confirmed	Doubtful____

cf., Null et al. 1993.

Knowledge of the orbit of Charon around Pluto, which is essential to understanding the dynamics of the system, densities of the bodies, and even the radius of Pluto (through stellar occultations) has been undergoing constant improvement since the satellite's discovery in 1978. The combination of the semi-major axis and orbital period provides the mass of the system, which when coupled with radii for the two objects yields the mean density of the system, the significance of which is described in Section 4 below. The orbital period is the easier of the two to measure. Accurate timings of mutual eclipse and occultation phenomena between Pluto and Charon during the orbit plane crossing of 1984-1990 yielded an orbital period of 6.38722 days. The semi-major axis is far more difficult to determine, requiring direct imaging of the system, which at maximum separation spans a mere 0.9 arcsec. Ground-based efforts to measure the semi-major axis are limited by atmospheric seeing effects, giving error bars in the 100-km range. Space-based observations with the Hubble Space Telescope (HST) are capable of higher spatial resolution now that the optics are repaired (Tholen and Buie, 1997). While Charon's orbit lies roughly in Pluto's equatorial plane, significant discrepancies remain in various determinations of the precise orbital inclination, presumably due to systematic errors in the calibration of the position angle for the major axis of the projected ellipse.

A recent development is the detection of a significant non-zero eccentricity in the motion of the center of light of Charon around the center of light of Pluto (Tholen and Buie, 1997). The two centers of light depend on the assumed surface albedo distribution, and although the eccentricity can be reduced by incorporating current albedo maps of the system, a significant non-zero value remains. Precise determination of the eccentricity can be achieved by a spacecraft flyby, either by direct imaging of the orbital motion of Charon about Pluto, or improvement in our knowledge of the surface albedo distribution (which allows more precise Earth-based tracking of the centroids of each object).

3. Bulk Parameters

3.1 Radii

Four different techniques have been used to measure the radii of Pluto and Charon: speckle interferometric imaging, stellar occultations, mutual events, and direct imaging with the HST Faint Object Camera. The speckle determinations suffer from assumptions about surface albedo distribution and limb darkening, are quite discrepant, and have the largest error bars of the four techniques. Because they are no longer competitive with the more recent measurements, we do not discuss them further.

Only two stellar occultations have been successfully observed, one for each body. The Charon occultation was seen from only a single site, hence the chord length provides only a lower limit of 601 km to the radius of Charon. The Pluto stellar occultation was observed from several sites, but the discovery of an atmosphere around Pluto makes radius determinations dependent on models of the atmospheric temperature profile (Elliot et al., 1989; Stansberry et al., 1994). Model radii for Pluto are in the 1180 to 1200 km range, with smaller values accommodated by assuming, for example, the presence of a troposphere.

The mutual event radius determinations rely on an accurate value for the semi-major axis of Charon's orbit to provide the physical scale. Although theoretically capable of the highest accuracy of the four techniques mentioned, some slight model dependencies remain, particularly due to the assumed limb darkening (Buie *et al*., 1992). The results place the radius of Pluto in the 1150 to 1160 km range, while Charon falls in the 590 to 630 km range (Albrecht *et al*., 1994).

Direct images by HST using the Faint Object Camera suffer from lack of knowledge about the limb darkening. Furthermore, Charon is barely resolved. In spite of these limitations, the results are comparable to those obtained from the occultation and mutual event modeling techniques (Buie et al., 1997).

A spacecraft flyby can provide accurate radii that are not limited by the limb darkening assumptions that afflict the techniques used to date, resulting in significant improvements in the radii of Pluto and Charon and hence in the derived densities.

3.2 Rotation

Rotational information for Pluto and Charon is based on accurate photometric observations extending over four decades. Because the light from the system is dominated by the light from Pluto, this information mainly tells us about the rotation rate and large obliquity (120°) of Pluto. Only recently have resolved observations from HST provided an indication of Charon's rotational properties. Dynamical arguments suggest that Pluto and Charon are tidally locked, and the available data do not contradict these arguments.

3.3 Densities

The limiting factor in our knowledge of the system mean density lies with the radii, which are discussed above. Of more interest, however, are the individual densities, which rely on knowing the mass ratio of the two bodies. Two attempts to measure this mass ratio in 1991 (HST) and 1992 (ground-based) yielded completely different results (Null et al., 1993; Young et al., 1994). Both sets of observations were repeated in 1993 (HST) and 1995 (ground-based), but it is too early to say whether the discrepancy will be resolved. At this point, all that can be said is that the system mean density is approximately 2.05 grams per cubic centimeter, with the individual density of Pluto being near this value, and Charon being as dense as, or somewhat less dense than, Pluto.

4. Internal Structure

Given the density, radius, and information on the rotational state of Pluto and Charon, along with basic data on the rheology of ices and rock, internal structure models of Pluto and Charon can be constructed. Because of the high cosmochemical abundances of water ice and silicates, these are assumed to be the predominant constituents. Figure 1 shows a resulting model for Pluto, from McKinnon et al. (1997). Models for the formation of Charon by impact of a large body into Pluto imply substantial heating of Pluto's interior, leading to softening of the ice and separation of the rock to form a core (this might well happen in any event as radioactive elements in the rock heat the interior and soften the ice). The same exercise can be performed for Charon, but the current uncertainty in its density prohibits definitive results.

Quantitative interior models permit an estimate of the mass fraction of rock, relative to ice, which is present in Pluto's interior. This can be compared to the fraction expected in a primordial mixture of rock and ice from which outer solar bodies were accreted (McKinnon and Mueller, 1988; Stern, 1988; Simonelli et al., 1989). As described in Stansberry et al. (1994), the current uncertainty in Pluto's radius prohibits a definitive result, but it appears that Pluto has a somewhat higher rock-to-ice ratio than predicted for primitive material. Loss of water early in its history, perhaps as a result of a Charon-forming impact, is a plausible explanation for the slightly rock-rich nature of Pluto (e.g., McKinnon, 1989). However, a more definitive determination of the radius is required before the amount of water loss can be estimated.

5. Albedo Markings

Next to Earth and Iapetus, Pluto has the largest global-scale surface contrast in the Solar System. Indeed, Pluto's rotational lightcurve shows brightness variations of about 0.35 mag (i.e., 30 percent disk-integrated brightness viewed equatorially), which provides the primary evidence for large-scale albedo variations over the surface of Pluto. The locations of those markings are further constrained by the way in which the lightcurve amplitude has increased over the years since precise photometry began in the mid 1950s. Models based on the assumption that the markings could be approximated by circular spots were developed by

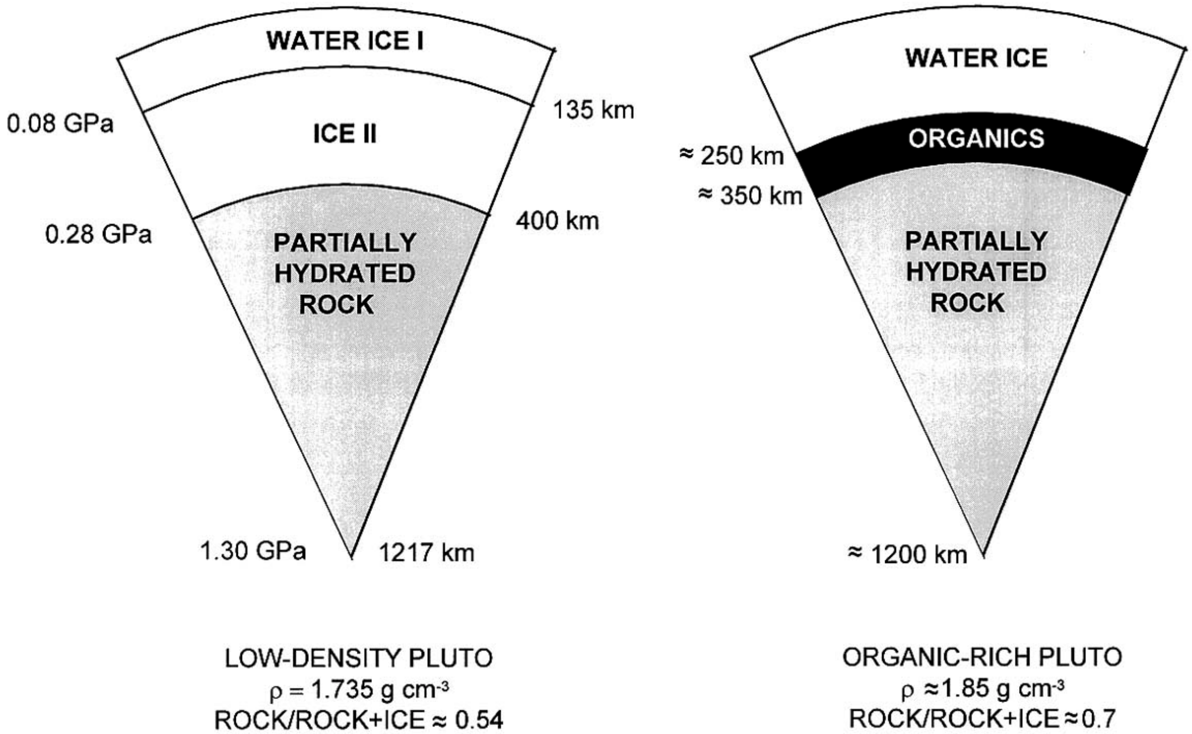

Figure 1: Two models of the interior of Pluto, shown in cross section; pressure in gigapascals shown on the left. Ice I and Ice II are low- and high-pressure phases of water ice, respectively. Figures from McKinnon et al. (1997).

Marcialis (1983), Buie and Tholen (1989), Young and Binzel (1993), and Reinsch et al. (1994).

Once Charon started occulting Pluto during the mutual event season of the 1980s, it became possible to map the locations of albedo markings with somewhat higher spatial resolution, but over only Pluto's Charon-facing hemisphere, due to the tidal lock between the two bodies. Models have been computed by Buie et al. (1992) and Young and Binzel (1993). They both show a bright south polar cap and a darker equatorial region.

Direct imaging with the repaired HST has provided a more definitive means of mapping out the locations of albedo features on Pluto, and although the spatial resolution is somewhat lower than for the maps based on mutual event observations, global coverage is possible. The first such observations show polar caps and large equatorial spots (Stern, 1997).

Charon is only barely resolved by HST, so once again we must rely on rotational lightcurve information to constrain the global albedo variation, given that the mutual event data also map out only one hemisphere of Charon. The lightcurve of Charon, as measured from HST, shows less than 0.1-mag variation, indicating a much more uniform surface (Buie et al., 1997).

As a function of wavelength, the albedo of Charon appears constant (i.e., gray) throughout the visible part of the spectrum, whereas Pluto's albedo increases with wavelength until the strong methane absorption features are encountered at near infrared wavelengths. At 0.44 μm, Charon's reflectivity is about 40 percent, while Pluto's surface varies in the 40 to 60 percent range over spatial scales comparable to the size of Charon. The contrast is presumably much higher over smaller scales.

6. Surface Composition and Physical State

Pluto's surface is covered with materials of diverse chemical composition and reflectivity. The discovery many years ago of the planet's changing brightness during its rotation demonstrated there is a non-uniform distribution of dark and bright surface materials on its surface and at the same time permitted the determination of the diurnal period of 6.3872 days.

The bright material on Pluto appears to consist primarily of solid nitrogen, with various other volatile molecules present as secondary frosts or mixed with nitrogen as a contaminant (Owen et al., 1993). Spectroscopic observations with Earth-based telescopes show that methane included in the N_2 constitutes approximately 1 percent (by mass), while carbon monoxide in the mixture contributes somewhat less than 1 percent of the large expanses of the solid N_2.

Molecular nitrogen ice tends to form large crystals in the laboratory and on Pluto might anneal and sinter into large semi-transparent expanses many meters in dimension. The detailed properties of the N_2-covered regions of Pluto's surface are not known, but the spectroscopic evidence suggests variation and complexity. It appears that some CH_4 is trapped in the N_2 and some is in separate patches on the surface, where it is exposed to the atmosphere. Similarly, some of the CO that has been detected may occur as exposed surface outcrops. Because of Pluto's diurnal and seasonal cycles, the distribution of the N_2 and its contaminants is probably variable on both short and long time scales. The profile of the N_2 spectral band suggests that the nitrogen on Pluto occurs in the β region of the α - β phase space (the transition temperature is 35.6 K) and that the temperature of the nitrogen ice is 40 ($\pm$ 2) K at the present near-perihelion epoch (Stern et al., 1993; Tryka et al., 1994; Jewitt, 1994). Temperature changes of the N_2 ice with season may take it below the phase transition temperature and into the α phase. αN_2 has a cubic crystalline structure of higher density than βN_2; transitions from one phase to the other may cause physical (or at least optical) disruption of the nitrogen ice on Pluto's surface.

In addition to the molecules so far identified on Pluto, the infrared spectra suggest that additional compounds remain to be found. In particular, other hydrocarbons may occur. Their spectral features are in part masked by the strong CH_4 bands, but efforts are underway to identify additional molecular species. Furthermore, isotopes of C, O, and N may be identified with higher spectral resolution measurements.

Those regions of Pluto not covered by N_2 have a lower albedo, a distinctly red color, and a higher temperature, as suggested by IRAS data (Sykes et al., 1987). Albedo maps of Pluto, as well as thermal models of the temperature distribution, suggest that the darker areas are near the equatorial regions, with polar caps composed (from ground-based spectra and analogy with Triton) of N_2 ice. The composition of the darker areas is not known, but it may include refractory organic solids produced by photochemistry of the molecules found in the ice (and in the atmosphere), material accreted from outside sources, or products of cosmic ray bombardment and photochemical processes. Finally, patches of nearly pure methane probably exist on the surface at elevated temperatures compared to the nitrogen frost (Stansberry et al., 1996).

Charon's surface is less reflective than Pluto's. Spectroscopic observations show that it is largely (if not entirely) covered by frozen water plus some unidentified gray (neutral colored) component that is nearly uniformly distributed across the satellite's surface (Buie et al., 1987; Marcialis et al, 1987). While the presence of H_2O is certain, additional ices could also be present. Quantitative models of the reflectance of Charon show that a large quantity of solid CO_2 and a substantial amount of CH_4 and CO on Charon are not excluded by the existing data; the exact amounts depend strongly upon the details of the scattering geometry (e.g., the dimensions of the grains) of the surface (Roush, 1994).

The presence of other volatile materials on both Pluto and Charon is of great interest in understanding the origin of these and other small bodies of the outer Solar System. The compositional relationship of this unique binary system to the neighboring Kuiper Belt of planetesimals bears on the origin and chemical evolution of the comets, the outer planets and their satellites. It is important that we establish the composition of the darker materials on both Pluto and Charon to learn if they are related to the organic materials imported to the Solar System from the nascent molecular cloud during formation or if they are produced over time on the surface by cosmic-ray bombardment or photochemistry.

The extreme seasonal cycle experienced by the Pluto-Charon pair affects the interaction of the surface volatiles and the atmosphere of Pluto. The interchange of material from surface solids to atmospheric gases during this cycle has been modeled theoretically but is not yet observationally constrained.

7. Pluto's Atmosphere

7.1 Some General Considerations

Information about Pluto's atmosphere comes from a variety of sources. Direct information was first obtained during the occultation of a 12th magnitude star by Pluto in 1988. Measurements of the composition and physical state of the surface also bear directly on the atmosphere because we believe that the composition and structure of the atmosphere is determined to a large degree by its interaction with the surface. Less direct information is obtained by comparing Pluto with Triton. Triton is roughly the same size as Pluto and likely formed in a similar orbit around the Sun (McKinnon, 1984; Goldreich et al., 1990). For these reasons, as well as because the atmospheres of both Triton and Pluto are predominantly N_2, *Voyager* observations of Triton should provide a good guide to the range of phenomena to be expected in Pluto's atmosphere. Finally, we can rely upon physical theories to help frame questions about Pluto's atmosphere, bearing in mind that specific predictions about the physical state of an unstudied atmosphere are difficult and likely to be unsuccessful. What we do know about Pluto suggests an atmosphere that is both varied and extreme in many ways. Because of the expected large variations in the surface temperature (a consequence of the observed albedo patterns and volatile distribution), the atmospheric structure near the surface is likely to exhibit large geographic variations. Horizontal temperature variations may be as large as a factor of two (on Earth a 10% variation is considered large). There are suggestions, based on the occultation data, that the vertical temperature gradient in the atmosphere could be as steep as 20-30 K/km. The atmosphere contains at least three condensable species, namely N_2, CO, and CH_4. The interplay between these atmospheric species and the associated surface ices should be complex, with an interesting analogy to CO_2 and H_2O on Mars. Pluto has the most weakly bound atmosphere in the Solar System and consequently the atmosphere that is lost most rapidly, relative to the atmospheric bulk.

When thinking about Pluto's atmosphere, it is important to remember that the knowledge based directly on observations is limited and that, in the history of outer Solar System exploration, nature has repeatedly demonstrated an imagination superior to our own. The atmospheres in the outer Solar System have proved to be more varied and interesting than predicted by earthly investigators. It is extremely unlikely, for example, that the geysers on Triton could have been predicted (or that such a prediction would have been taken seriously by the scientific community). The same is likely to be true of Pluto. Planetary exploration remains an observational science, and a mission is needed in order to understand Pluto. The description below follows this point of view.

7.2 Thermal Structure and Composition

In 1988 Pluto occulted a 12th magnitude star (Hubbard et al., 1988; Elliot et al., 1989; Elliot and Young, 1991; Millis et al., 1993). Our knowledge of Pluto's atmosphere is based largely on observations of this event. The occultation and its implications have recently been reviewed by Yelle and Elliot (1995). A brief summary is given here. The occultation was observed by several ground-based and airborne observatories. Although much can be learned from the simultaneous analysis of the entire occultation data set (Millis et al., 1993), the data obtained with NASA's Kuiper Airborne Observatory (KAO) have the highest signal-to-noise ratio and supply most of the basic information on the state of the atmosphere. The data along with model fits are shown in Figure 2. Both ingress and egress occultations were observed, and to within the accuracy of the data, the light curves appear to be identical. The occultation observations probe the atmosphere in the pressure region from several microbars to several tenths of a microbar, and within this region there are clearly some changes in the structure of the atmosphere. An abrupt change in the slope of the light curve occurs at 1215 $\pm$11 km, where the pressure is 2.33 $\pm$ 0.24 μbar. The nature of this change is discussed further below.

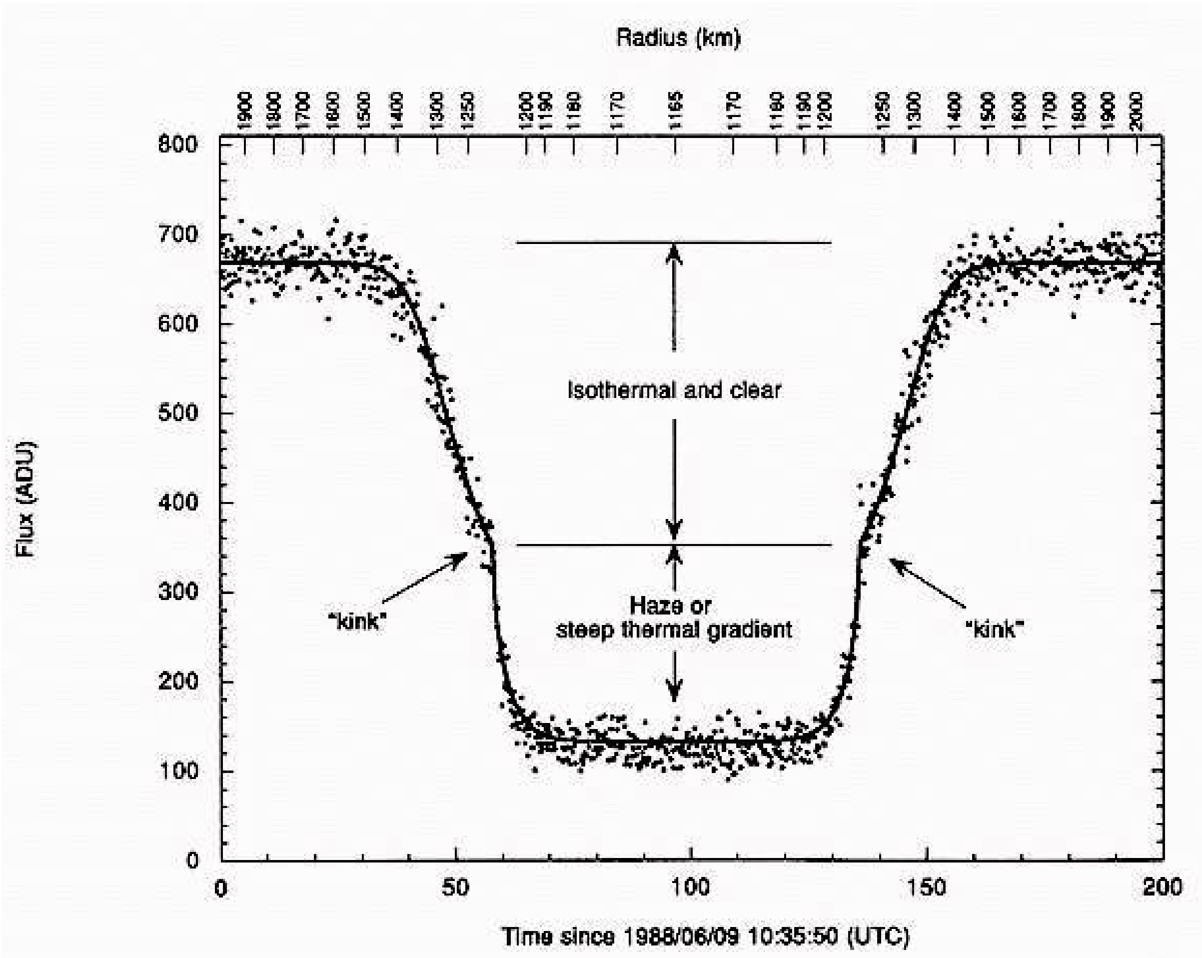

Figure 2: Data from the KAO observations of the 1988 occultation. The regions of the occultation well fit by an isothermal model and the location of the "kink'' in the lightcurve are indicated on the figure.

We first describe the atmosphere above 1215 km, because the structure in this region appears to be fairly simple.

Middle atmosphere

The occultation is sensitive to the ratio of temperature to mean molecular weight, T/μ, which is directly proportional to the atmospheric scale height. Analysis of the KAO data at altitudes above 1215 km implies a value of $T/\mu = 3.63 \pm 0.33$. Because of the similarity of the ingress and egress light curves, either this region of the atmosphere is globally uniform, or the occultation, by happenstance, probed two separate regions with identical temperature profiles. Moreover, the temperature in this region appears to be approximately constant with altitude. The KAO data have been used to constrain the temperature gradient to be 0.05 ± 0.07 K/km/amu. To determine the temperature of the atmosphere, it is necessary to know the mean molecular weight. There are two lines of reasoning that strongly imply that the atmosphere is predominantly composed of N_2. First, the atmosphere of Pluto is evolved from ices on its surface (Trafton and Stern, 1983). There is spectroscopic evidence for surface deposits of CH_4, N_2 and CO ice. Owen et al. (1993), from spectroscopic data, determined that N_2 is the dominant ice on Pluto's surface. At the relevant temperature, N_2 has a vapor pressure an order of magnitude larger than CO and several orders of magnitude larger than CH_4; thus, as the most volatile and abundant ice on the surface, it appears certain that N_2 will dominate the atmosphere, and the mean molecular mass should be close to 28. Tryka et al. (1994) have used the temperature dependence of the N_2 band shape to estimate a temperature for the surface ice of 40 ± 2 K. This implies a surface pressure of 19-160 μbars. Although this is not a strong constraint on the surface pressure, it does imply that the N_2 ice on the surface is warm enough to support a significant atmosphere. The depth of the atmosphere is discussed further below.

Second, a mean molecular weight of 28 implies an atmospheric temperature of 102 + 9 K. This value is close to the CH_4 radiative equilibrium temperature calculated by Yelle and Lunine (1989), suggesting that the atmosphere contains enough CH_4 to control the thermal structure (Yelle and Elliot, 1995). The CH_4 abundance required for this is on the order of 1% (Yelle and Lunine, 1989; Strobel et al., 1996). Lellouch (1994) points out that cooling by CO could be important and argues that the CH_4 abundance is small; he suggests that the elevated temperatures are due to aerosol heating. Young (1994) has inferred the column abundance, η, of CH_4 in the atmosphere through analysis of high-spectral-resolution measurements of CH_4 absorption bands in the near-infrared region of the spectrum. She determines a value $\eta = 1.2$ (+3.15, -0.87) cm-amagat, which corresponds to a CH_4 partial pressure of 9.8 (+2.5, -0.7) x 10^{-2} μbar. Since the N_2 abundance in the atmosphere is not well known, it is not possible to tightly constrain the CH_4 mole fraction. Clearly, determination of the relative abundances of N_2, CH_4, and CO is critical to an understanding of the thermal structure of Pluto's atmosphere. At the present time, there are no direct observations of CO in Pluto's atmosphere. CO ice does reside on the surface, however (Owen et al., 1993), and therefore CO should be present in the atmosphere also. The abundance is difficult to predict with the data available. On Triton, the atmospheric CO is undersaturated by several orders of magnitude, probably because the CO ice is bound in an N_2 matrix (cf. Yelle et al., 1995). Argon and other noble gases are cosmically abundant and sufficiently volatile to be present in Pluto's atmosphere if their ices exist on the surface. Because of the lack of spectral features, upper limits on the possible abundance of these ices are not available.

Lower Atmosphere

The atmospheric structure below 1215 km is more complicated and less well understood. Elliot et al. (1989) suggested that the change in slope of the light curve could be due to the abrupt onset of an aerosol layer at 1215 km; Eshleman (1989) and Hubbard et al. (1990) suggested that the break in the light curve could be due to a strong temperature gradient in the atmosphere, such as that present in the thermal inversion model of Yelle and Lunine (1989). In either case the lower atmosphere of Pluto is obscured, and the net result is that the surface pressure of Pluto's atmosphere is poorly constrained. Stansberry et al. (1994) demonstrate that a troposphere, i.e. a near-surface atmospheric region with a negative temperature gradient, of up to 40 km deep would not produce noticeable effects in the occultation data. Therefore, it is possible that the surface of Pluto lies many tens of kilometers below the level probed by the occultation. The best upper limit on the surface pressure comes from the temperature determination of Tryka et al. (1994); their warmest temperatures correspond to a surface pressure of 160 μ bar; thus, the surface pressure lies between roughly 3 and 160 μ bars. Since the surface is much colder than the atmospheric temperature of 100 K, there must be a region of strong positive temperature gradient. The shape of the temperature profile is not known at the present time. It is likely that there are geographic variations in the near surface vertical temperature profile related to the observed albedo variations on the surface, but there are no observational constraints on these variations.

The structure of Pluto's lower atmosphere is an outstanding question. If the change in slope of the KAO light curve at 1215 km is due to a temperature gradient, then the gradient is likely to be large. Stansberry et al. (1994) estimate that a gradient of 20 K/km is required, although this value depends on the assumed shape of the temperature profile. Similarly, if the change in slope is due to aerosol absorption, the aerosols are far more abundant than expected (cf. Yelle and Elliot 1995) posing a different puzzle. Even our limited knowledge of Pluto's atmosphere is sufficient to distinguish it among atmospheres in the Solar System.

The surface pressure, though ill-determined, is on the order of tens of microbars, which places it in the same class as Triton's atmosphere. Though small, this surface pressure is sufficient to support a host of interesting and observable physical processes in the atmosphere. However, Pluto's atmosphere appears to be under radiative control, at least in the 1 μbar region, which is very different from Triton, whose lower atmosphere is essentially at the same temperature as the surface. The large discontinuity between the surface temperature and atmospheric temperature is unique in the Solar System, and it is very unlikely that all of the implications of this situation are understood at the present time.

7.3 Atmospheric Chemistry

In addition to the species supplied by the evaporation of surface ices, Pluto's atmosphere should contain molecular, atomic, and ionic species produced by photochemistry. The situation should be similar to that on Triton, with important differences due to the larger CH_4 abundance, potentially different CO abundance, distinct energetic particle environments, and disparate atmospheric temperatures. The chemistry of Triton's atmosphere has proved to be complex (cf. Summers and Strobel, 1995). The main feature is a very close connection between the neutral photochemistry of the lower atmosphere and the ion-neutral chemistry in the ionosphere. The presence of CH_4 and N_2 in the atmosphere implies the presence of photochemically produced species such as H, N, HCN, C_2H_4, along with other hydrocarbons and nitrides. Photochemical model calculations for the abundance of minor constituents have been presented in Summers and Strobel (1995). These exploratory calculations are a useful way to study the physical and chemical processes in Pluto's atmosphere. However, there are a lack of observational constraints on the minor constituents, uncertainties in basic atmospheric parameters such as surface pressure, bulk composition, vertical mixing rates, aerosol content, etc., and uncertainties in the values of reaction rates at low temperature. In consequence, a wide range of results is possible, and the models do not have much predictive capability. Nevertheless, although the abundance of minor constituents cannot be predicted with confidence, the Summers and Strobel models probably do provide a good guide to the types of minor constituents likely to be in the atmosphere. An illustrative calculation, showing density profiles for some of the photochemically produced species, is presented in Figure 3.

Pluto presents another example of an interesting problem in the evolution of volatile atmospheres in the outer Solar System. CH_4 is irreversibly lost from the atmosphere because photolysis liberates H and H_2, which rapidly escape. The loss rate for atmospheric CH_4 due to photolysis is on the order of ten thousand years, much shorter than the age of the Solar System. Either the initial endowment of CH_4 ice on Pluto's surface is sufficient to resupply the atmosphere over the age of the Solar System, or CH_4 must be supplied from a reservoir in the interior. If the latter possibility is correct, it implies the existence of geological processes that transport CH_4 from a subsurface reservoir to the surface. Another consequence of photolysis is the production of higher order hydrocarbons (such as those predicted by the chemical models mentioned above) that eventually condense and end up on the surface, yet no other hydrocarbon species have been detected. These same questions appear in slightly different guises on both Triton and Titan. More thorough searches for photochemical products are required, and the theoretical mechanisms of photochemistry in the atmosphere need to be observationally tested.

7.4 Atmospheric Circulation and Volatile Transport

Because Pluto's atmosphere is evolved from ices on its surface, volatiles are transported through the atmosphere in response to diurnal and seasonal changes in solar insolation. These winds are thought to carry sufficient energy to maintain the surface deposits of N_2 ice at all locations on Pluto at a single common temperature (Trafton and Stern, 1983; Spencer et al., 1995). Groundbased maps of Pluto exhibit a bright region near the southern pole (Young and Binzel, 1993; Buie et al, 1997); it is tempting to identify this feature with a polar cap of N_2 ice. There are also dark regions on the surface, which are probably devoid of N_2 ice.

The N_2 deposits on Triton should migrate over the surface of the body in response to seasonal forcing. Understanding the albedo patterns on Triton's surface has proved difficult, although a number of physical processes have been identified (cf. Yelle et al., 1995). Studies have been hampered by the lack of information on compositional variations across the surface: *Voyager* carried no instruments capable of spectroscopic determination of surface ice composition, and therefore composition had to be inferred from the visible albedo with very ambiguous results. This will not be a limitation on Pluto-Kuiper Express given the spacecraft strawman payload. There have been several preliminary (necessarily theoretical) studies of volatile transport on Pluto (Hansen and Paige, 1996; Spencer et al., 1995). The goal of these studies is to understand the distribution of volatiles on the surface through the study of seasonal transport

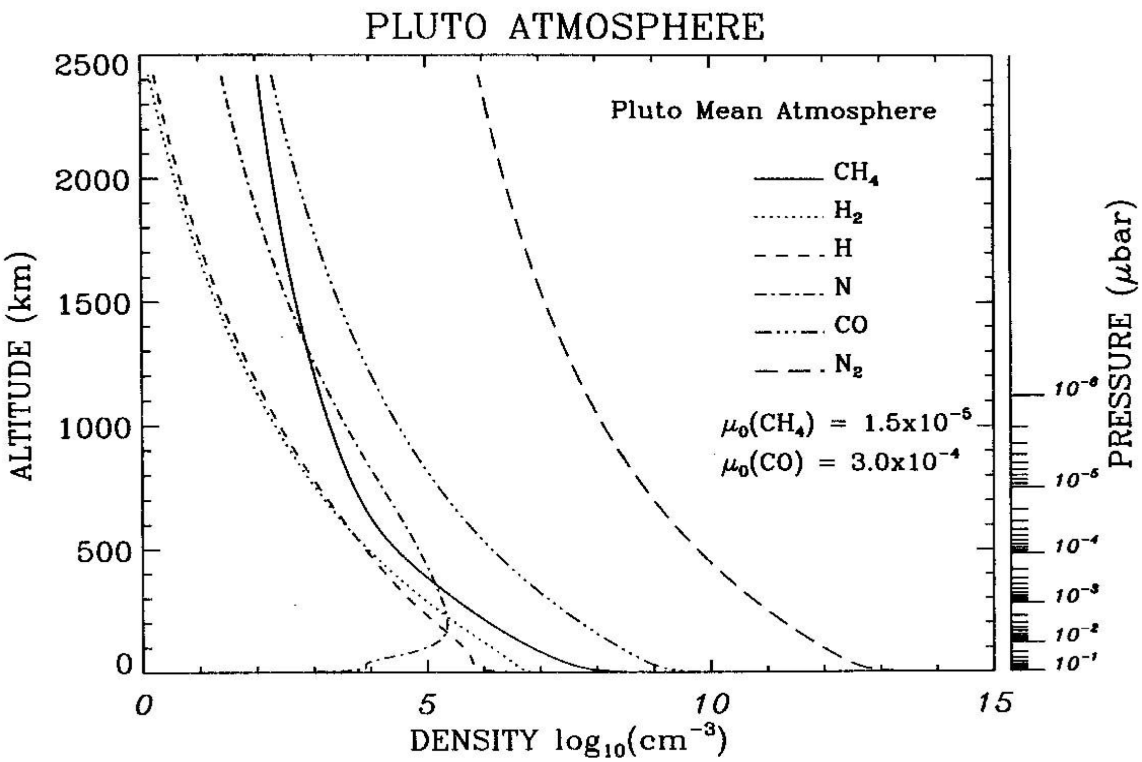

Figure 3: Calculations of the composition of Pluto's atmosphere from Summers and Strobel (1995). These photochemical calculations assume that the atmosphere is predominantly N_2 with small amounts of CH_4 and CO; the distance of Pluto from the Sun is set at 40 AU, yielding a surface pressure less than that derived from the 1988 stellar occultation, which occurred near perihelion.

processes, i.e. to understand the formation of polar caps. One of the difficulties faced by studies of Pluto's seasonal cycles is that it has proved difficult to understand the apparently complex distribution of volatiles on Triton revealed by *Voyager 2*.

Despite the present difficulties in understanding the volatile distribution on Triton, several signatures of seasonal transport processes are evident. Wind streaks were observed on the surface at virtually all locations in the southern hemisphere (Hansen et al., 1990). The streaks were oriented predominantly to the northeast, which is consistent with the direction expected for seasonal volatile flow near the surface. Several different types of cloud features were observed in the atmosphere, and in several cases the movement or orientation of the clouds allowed the inference of wind directions (Hansen et al., 1990). Consideration of all of these data along with some simple dynamical concepts has resulted in a fairly complete description of Triton's circulation patterns (Ingersoll, 1990; Yelle et al., 1995). It is possible and probably likely that the same types of signatures will be evident on Pluto's surface and in the atmosphere.

7.5 Cloud Formation and Aerosols

For the purposes of discussion, we define clouds as particulates in the atmosphere created by the condensation of one of the major atmospheric species; thus, clouds on Triton probably consist of N_2 ice, and clouds on Pluto could consist of CH_4, CO, or N_2 ice. Hazes may be formed by photochemical processes in the atmosphere, similar to those that on Earth produce smog in major urban centers. Although condensation of a photochemical product species is probably responsible for the creation of aerosols, the particulates so formed differ in character from those formed by condensation of a main constituent. At least that seemed to be the case on Triton, where *Voyager 2* saw clearly defined discrete clouds scattered over the southern hemisphere and a pervasive diffuse haze that permeated the entire atmosphere except for one particular and curious location (cf. Yelle et al., 1995). All of the atmospheres in the outer Solar System contain hazes, and Pluto should be no exception. As mentioned above, the hazes are believed to be photochemical in origin (Elliot et al., 1989), but further study is required to determine the mechanism by which the hazes form, the potential for supersaturation, and the role of aerosols in photochemistry. If Pluto possesses a troposphere, as suggested by Stansberry et al. (1994), then it is likely that clouds also form. The repeatability of Pluto's rotational lightcurve argues against a thick planetwide cloud layer (i.e. Venus like), but clouds of the type observed in Triton's atmosphere could be present.

7.6 Temporal Variations in the Atmosphere

Temporal variations in Pluto's atmosphere are potentially very large, because the large eccentricity of its orbit carries it from 29 to 49 AU, which corresponds to a 41% drop in insolation from perihelion to aphelion. If, for example, Pluto is assumed to be covered with N_2 ice with an albedo of 0.8, and it is further assumed that the emissivity of the ice has a value of 0.75, which is constant with temperature, then the surface temperature should vary from 34-42 K, and the surface pressure should vary from 1-40 μbar from aphelion to perihelion (Stern et al., 1993). Stansberry and colleagues at NASA Ames have argued that changes in the emissivity of surface nitrogen ice as it undergoes a low-temperature phase transition could buffer the atmosphere and prevent substantial collapse (Figure 4). It is clear from both theory and observation that the temporal behavior of Pluto's atmosphere is poorly understood and might be complex.

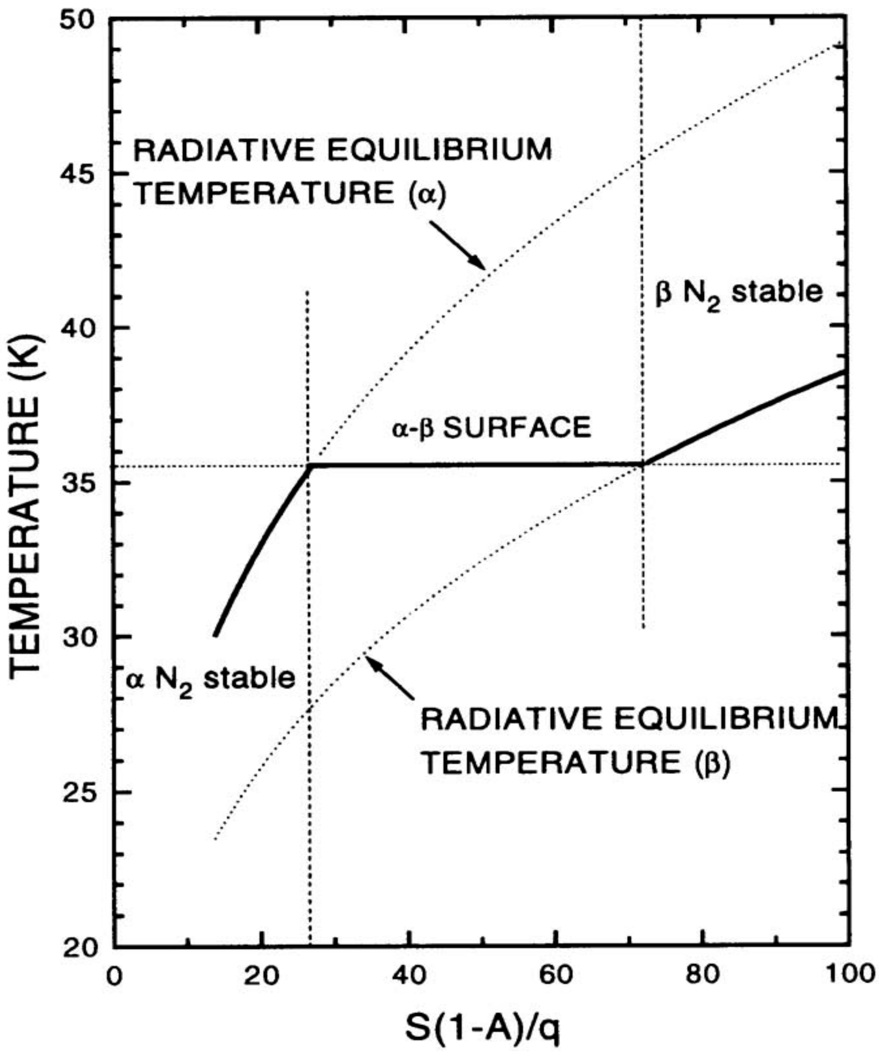

Figure 4: An example of a possible buffering of Pluto's atmosphere by surface ices, from John Stansberry at NASA Ames and colleagues. Plotted is radiative equilibrium temperature versus absorbed solar insolation (here S is solar flux, A albedo, and q a factor associated with the distribution of reradiated solar flux). The two different nitrogen phases, α and β N_2, have differing emissivities and hence different radiative equilibrium curves. Because of this, a possible buffering of the surface temperature around the phase transition temperature (35 K) is possible.

It is equally clear that, as Pluto moves away from perihelion, the next couple of decades are an important, perhaps crucial, time to study any atmospheric changes that might take place. Should Pluto's atmosphere decrease in mass over time, its various properties could change dramatically, as suggested in Figure 5, prepared by M.S. Summers (unpublished).

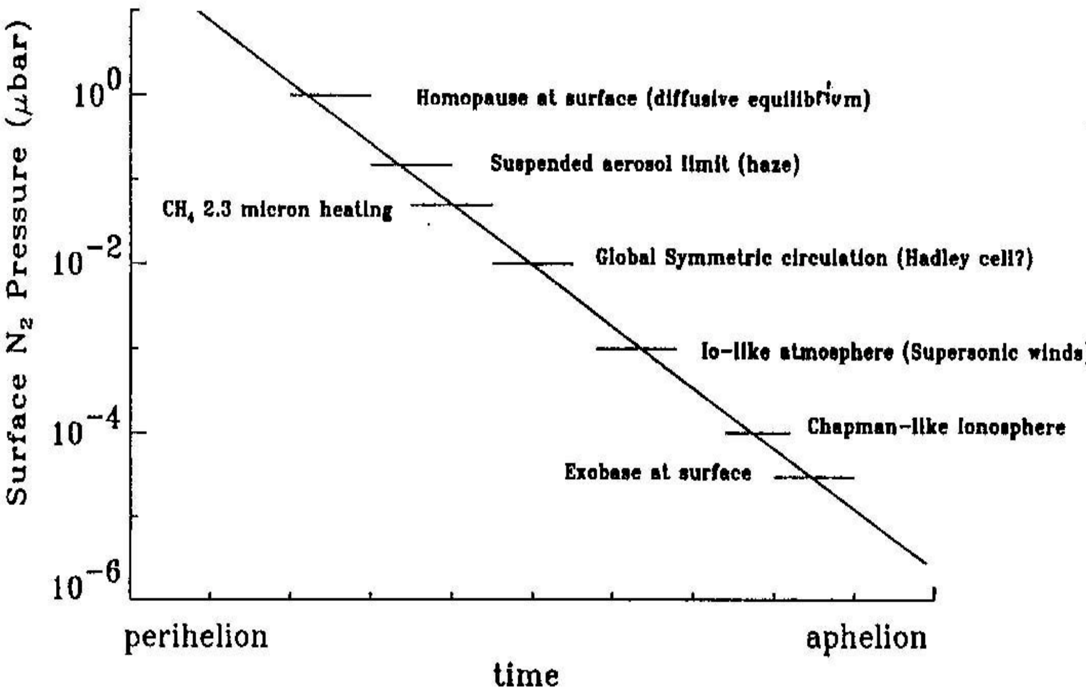

Figure 5: Changes in the characteristics of Pluto's atmosphere based on a possible decrease in its size as Pluto moves toward aphelion. Key to each of the threshold levels: Homopause is the level at which molecular species separate according to mass; CH_4 heating refers to the minimum density at which methane is an effective near-infrared absorber; Hadley cell and Chapman-like ionosphere are described at length in Chamberlain and Hunten (1987); exobase is the level at which the atmosphere becomes collisionless. Figure prepared by M.S. Summers.

7.7 Atmospheric Escape

As a consequence of its relatively small size and relatively high atmospheric temperatures, Pluto has the most extended and most weakly bound atmosphere in the Solar System. In a hydrostatic atmosphere, the variation of pressure with altitude is governed by the ratio of gravitational potential energy to kinetic energy, λ=GMm/kTR. On Pluto, the value of lambda inferred from the occultation is 22.4 $\pm$ 0.8, nearly a factor of 3 smaller than for any other atmosphere. This implies that Pluto will have a greatly extended atmosphere that is rapidly escaping to space. In particular, the hydrostatic approximation no longer applies because outflow velocities are large enough that inertial terms in the momentum balance equation are important. The outflow has the effect of cooling the thermosphere to temperatures below that which would occur in a hydrostatic case. Jean's equation for the atmospheric escape rate is not valid for Pluto, and the hydrodynamic equations must be solved to determine the atmospheric structure and the escape rate.

Although hydrodynamic escape is believed to be an important process in the evolution of many atmospheres, Pluto represents the only non-hydrostatic atmosphere in the present day Solar System, and we have a unique opportunity to study this phenomenon.

8. The Interaction of Pluto With the Solar Wind

Pluto is similar to Triton in mass, radius, and, currently, surface pressure (Stern, 1992). However, Triton's atmospheric structure and plasma environment are quite different, and the thermal escape rate is negligible. The surrounding plasma environments are also quite dissimilar. In spite of the *Voyager 2* flyby through the Neptune system, the nature of the interaction of Triton with its plasma environment was not established due to lack of a close/downstream approach by the spacecraft (Neubauer et al., 1991), although a substantial ionosphere was detected (Tyler et al., 1989; Majeed et al., 1990; Strobel et al., 1990).

Titan, the other small world with a substantial atmosphere, is known to interact with the plasma in Saturn's magnetosphere (McNutt and Richardson, 1988 and references therein). Again there are substantial differences from Pluto, and at the current epoch, the interaction of Pluto with the solar wind plasma is truly unique in the Solar System.

The primary difference between Pluto and these other worlds is the suspected high escape rate of Pluto's atmosphere. This hydrodynamic escape is powered at least partly by the mesospheric absorption of solar EUV and FUV radiation and potentially has significant consequences for the interaction of Pluto with the solar wind (precipitation of charged particles could also play a role in powering the atmospheric escape). The nature and extent of the interaction has, in turn, consequences for atmospheric evolution and possible surface effects.

The extreme cases of the interaction of the solar wind with neutral atmospheres range between a gravitationally bound atmosphere, e.g. Venus (Luhmann, 1986), and a freely evaporating atmosphere such as found during spacecraft encounters with comets (Neugebauer, 1990). In the former case, an ionosphere is present, and the interaction is governed by ionospheric chemistry and dynamics. In the latter case, the interaction is through the mass loading, deceleration and deflection of the solar wind via ionization and subsequent pick-up and gyration of the outflowing neutrals.

The idea of an atmosphere of Pluto (Trafton, 1980) was only recently settled by the stellar occultation of 1988 (Hubbard et al., 1988; Elliot et al., 1989). The inferred hydrodynamic escape of Pluto's atmosphere (McNutt, 1989 and references therein) suggests Pluto resembles a "heavy comet" with significant mass-loading of the solar wind over an extensive region around the planet (Bagenal and McNutt, 1989; Kecskemety and Cravens, 1993). The "break-point" for the comet analogy can be estimated from fluid theory (Galeev et al., 1985) as a mass loading rate of 1.5×10^{27} molecules s^{-1} (Bagenal and McNutt, 1989). If the true escape rate is much less than current estimates of 2.3×10^{27} to 3.4×10^{28} molecules s^{-1}, Pluto's ionosphere could deflect the solar wind in a Venus-like interaction confined to a region much closer to the planet.

Depending upon the exact nature of this interaction, measurements of the solar wind/Pluto-ion interaction region can yield a sensitive measure of the escape rate of Pluto's atmosphere and whether or not it is in a state of supersonic hydrodynamic escape. The accuracy of this determination will depend itself upon the nature of the interaction (comet-like, Venus-like, intrinsic magnetic field - see below).

The gyroradii of both solar wind ions and picked-up atmospheric ions will be very large due to the weak interplanetary magnetic field (0.1nT) at 30 AU. The gyroradius for methane pick-up ions near Pluto is β 500 R_{Pluto}. Molecular nitrogen ions (or carbon monoxide ions) will have pick-up gyroradii roughly twice as large.

The thickness of an upstream bow shock would be >10 R_{Pluto}, comparable to the size of the interaction region. With this scaling, a distinct bow shock is unlikely, and kinetic effects must be included in order to model the solar wind interaction realistically. In fact, the gyroradii are sufficiently large compared with the size of Pluto that the interaction is probably unique in comparison with all cases studied before except for the active AMPTE-ion releases in the solar wind. This situation is actually quite different from a cometary case at 1 AU with a high gas production rate such as at comet Halley, and the break point estimated above may also change substantially in the Pluto case. Theoretical work suggests that no bow shock forms due to the kinetic features of the interaction (Sauer et al., private comm.).

Given our lack of knowledge of the interaction, we can at least get a feel for possible scenarios by using some concepts from fluid theory.

As the solar wind flow penetrates the escaping neutral outflow, local ionization and subsequent pick-up decelerates the solar wind, leading to stagnation when the newly picked-up cometary ions dominate the composition. In the cometary plasma region the flow speeds are reduced to a km s^{-1}, the magnetic field is compressed, collisions become increasingly frequent and charge-exchange cools the plasma. Near the planet the gyroradii will decrease somewhat as the magnetic field is compressed by the "obstacle" formed by the pickup process.

For methane and typical parameters, the scale length for a fluid-like standoff region is

$$\frac{R_{so}}{R_{pluto}} = \frac{Q_{esc}}{Q_o}$$

where $Q_o = 1.5 \times 10^{27}$ molecules s^{-1}. Inclusion of charge exchange and impact ionization will make R_{so} larger. Thus, an escape rate $>10^{28}$, which would be comparable to the outgassing of Comet Giaccobini-Zinner at 1 AU (Mendis et al., 1986) and consistent with upper limits derived by Hunten and Watson (1982), Hubbard et al. (1990) and the more optimistic cases of McNutt (1989), would produce R_{so}~ 6 R_{Pluto}.

Drawing further upon the comet analogy, consider the pickup of CH_4^+ produced by the photoionization of methane outgassing from Pluto. In the transition region at distances >10^4 km from Pluto, pickup ion densities can be as high as β $10^{-4}cm^{-3}$, distributed in partial shells in velocity space. Corresponding energy spectra may exhibit differential fluxes greater than 10 $cm^{-3}s^{-1}keV^{-1}$ (Kecskemety and Cravens, 1993).

If the atmospheric escape flux is less than $1.5x10^{27}$ molecules s^{-1}, then the solar wind will interact more directly with the planet's atmosphere, similar to the cases at Venus and Mars and to the magnetospheric interaction with Titan. The Venus case is the best-studied because of the extensive Pioneer Venus data, but the cases of Mars or Titan are probably more appropriate analogies.

Pluto's ionosphere may resemble that of Triton in the absence of magnetospheric electron input (e.g. Ip, 1990). The expected ionospheric pressure is small, but it is comparable to the ram pressure of the solar wind at 30 AU. Thus, one expects a large interaction region compared with the size of the planet, with $R_{ionopause}$ > 1.5 R_{Pluto} (for the Titan-like case). This is actually more reminiscent of Titan where $R_{ionopause}$ = 1.4- 1.8 R_T and Mars (where $R_{ionopause}$ > 1.15 R_M). In this scenario, scavenging of the atmosphere by the solar wind may be significant over the lifetime of the Solar System.

In an exploratory mission one cannot *a priori* rule out surprises. Pluto could possess an intrinsic magnetic moment capable of standing off the solar wind. A surface field of only β=10 nT would suffice to stand off the solar wind (average conditions) to the exobase. Magnetization comparable to that found in some meteorites could lead to a convection-dominated magnetosphere that stands off the solar wind at several Pluto radii above the surface.

For a magnetosphere to extend to Charon's orbit at 17 $R_{Pluto,}$ the surface field must be B_o > 3700 nT. Such a hypothetical magnetosphere could be similar to that of Mercury (Russell et al., 1988) but with no belts of trapped radiation and plasma flows induced by the magnetic interaction with the solar wind. The presence of radiation belts and accelerated particles remains problematic in this scenario. Given the low power input available from the solar wind at such large heliocentric distances, it is not clear to what extent magnetospheric particles could be energized (Kivelson, private comm., 1993); cosmic ray albedo neutron decay particles may be present, at least.

For example, the asteroids Gaspra and Ida encountered by the Galileo spacecraft on its way to Jupiter are intermediate in size between the local electron and ion gyroradii. The resulting interaction with intrinsic asteroidal magnetic fields should be whistler-like.
Such signatures may have been actually detected by the Galileo magnetometer (Kivelson et al., 1993). This magnetosphere would persist throughout Pluto's orbit, even if Pluto's

atmosphere freezes out as it approaches aphelion. Any remnant magnetization of Charon is likely to be less than that of Pluto due to the relative sizes. Charon is likely to either be exposed directly to the solar wind flow or to a plasma modified by the interaction of Pluto with the solar wind.

Bombardment of methane ice by energetic (10 keV to 100 keV) protons leads to carbon enrichment, and hence darkening of the ice-bearing material, for fluences greater than 10^{16} cm^{-2} charged particles. Such irradiation has been suggested to be responsible for the dark color of the moons and rings of Uranus (Lanzerotti et al., 1987). The coloration of both Pluto and Triton suggests irradiated ice cover on the respective surfaces with color persistence suggesting resurfacing on time scales similar to those required for accumulation of a 10^{10} erg cm^{-2} charged particle dose; differences in the Pluto and Triton spectra suggest the visibility of a greater amount of irradiated material at Pluto (Thompson et al., 1987).

If Pluto undergoes a comet-like interaction, pick-up ions will be produced in the upstream solar wind, which can impact Pluto's atmosphere. (If the interaction region is sufficiently large they will also impact Charon). Actual production of color changes at the surface is problematic; the energies of the ions are probably not sufficient to penetrate the atmosphere and reach Pluto's surface at this time. As the outgassing rate decreases, penetration of ions to the surface will increase, but their intensity will drop. If Pluto possesses an intrinsic magnetosphere, then sufficient fluxes of energetic ions and electrons may be present to affect the surface color depending upon the particle energies reached (Johnson, 1989).

Scavenging of the atmospheres/surfaces of Pluto and/or Charon may be significant over Solar System time scales. If Pluto's atmospheric escape rate is low, then Charon is embedded in the solar wind, receiving 2×10^4 - 2×10^6 protons cm^{-2} s^{-1} (of kinetic energy $>$1 keV). For expected atmospheric escape rates from Pluto, pick-up fluxes at Charon's orbit could be about 10 kg of sputtered water over the course of a year. This additional source of material would contribute to the local mass loading and general escape of material from the Pluto/Charon system.

Voyager and Pioneer measurements show that in the outer heliosphere the solar wind seems to settle into a steady pattern of a strong stream lasting a few days and repeating each 26-day solar rotation period (Belcher et al., 1993). For a steady atmospheric escape flux (say 10^{28} s^{-1}), the corresponding 1σ variation in the size of the comet-like interaction region R_{so} is > 3.9 to 24 R_{pluto} for time scales of a few days (comparable to Pluto's rotation and Charon's orbital period of 6.4 days). This effect may be amplified or softened as the variations of EUV forcing of the upper atmosphere change the atmospheric escape flux on a similar timescale. If the atmospheric escape flux is low and the solar wind impinges directly on the ionosphere, then the size of the interaction region will also change in response to the solar wind ram pressure, though less dramatically than in the cometary case (because, effectively, the ionosphere is much less compressible).

Perhaps the most intriguing aspect of the Pluto/Charon system is the possibility of major changes over the 248-year orbital period due to the high orbital eccentricity. If the atmosphere does not completely freeze out, it will still undergo radical compositional changes. A very weak atmosphere (either now or as the planet recedes from perihelion) could lead to complete absorption of incident plasma, as at the Moon, and the production of a sputtered exosphere. If Pluto has a strong magnetic field (B_o> 3700 nT), then a magnetosphere will remain around Pluto and Charon throughout their orbit. In the absence of a significant intrinsic magnetic field, the solar wind interaction at Pluto might undergo a transition from "cometary" to "planetary" to "lunar" behavior as the escape flux decreases. If the interaction scale for the cometary interaction always exceeds that for an ionospheric interaction and the ionosphere ceases to provide adequate thermal pressure as the mass-loading weakens on receding from the Sun, then the Pluto interaction may evolve directly from comet-like to Moon-like.

Regardless of which, if any, of these scenarios and inferences is correct, the interaction of Pluto with the solar wind is likely to be unique in the Solar System. Given what little we do currently know about the atmosphere, detection and characterization of the interaction region at the current epoch will provide good estimates of the overall atmospheric escape rate and implications for the evolution of the Pluto/Charon system.

9. Kuiper Belt Objects and Pluto's Relationship to Them

Recently, trans-Neptunian bodies have been discovered that are widely believed to constitute the long-sought *Kuiper Belt*. This is a primordial disk of planetesimals beyond Neptune, which has survived since the formation of the planetary system. The Belt is of scientific interest on many levels. It is the suspected source of the short-period comets. Trans-Neptunian objects may contain some of the least processed Solar System material, and thus ultimately provide a window on processes operative in the epoch of planet formation. Mutual collisions in the Kuiper Belts of other stars are suspected sources of circumstellar dust, perhaps providing a link with such systems as the unexpectedly dusty main-sequence star *β Pictoris*. Collisions in our own Kuiper Belt may also be a source of observable dust; COBE (Cosmic Background Explorer) data are being independently analyzed in search of the anticipated low-temperature diffuse thermal emission.

The discovery of the trans-Neptunian objects of the Kuiper Belt, coming on the heels of the *Voyager* explorations of the giant planets and their satellites, has sparked continued scientific vigor in the study of the deep outer Solar System and provided grist for the mills of those interested in the origin of such disparate entities as Pluto, Triton, the Centaurs (the type member of which is the asteroid 2060 Chiron), comets and the planetary system itself. In addition to extensive observational efforts on moderate to large aperture telescopes, several theoretical studies have been sparked by the discovery of the Belt.

The remarkable orbital similarity between Pluto and some of the newly detected objects has provoked new work on the origin of that planet. Dynamicists are beginning to address the mechanism of capture into the 3:2 mean-motion resonance with Neptune. One result of the new work is the necessity to understand the relationship of Pluto to the smaller trans-Neptunian objects. Further, the Kuiper Belt is a dynamically plausible source for short-period comets, opening the possibility of a link between large outer Solar System solid bodies (such as Pluto and Triton) and short-period comets as the planetesimals from which they formed.

The key features of the Kuiper Belt are:

At the time of writing, 28 trans-Neptunian bodies exceeding 100 kilometers diameter (in addition to Pluto and Charon) have been directly observed from ground-based telescopes, all with low inclination orbits and small to moderate orbital eccentricities (Jewitt and Luu, 1993, 1995). Additionally, a population of smaller, perhaps comet-sized bodies moving consistent with Kuiper Belt orbits has been reported using Hubble Space Telescope data.

The orbits of many trans-Neptunians cluster near the 3:2 mean-motion resonance with Neptune at a = 39 AU. It is likely that these objects are stabilized against Neptune perturbations by the resonance, much like Pluto. Other objects (e.g. 1995 DA2 and 1995 DB2) may be in the 3:4 resonance, although further astrometry will be needed to prove this.

The total number of Kuiper Belt objects larger than 100-km diameter in the 30 AU to 50 AU heliocentric distance range is about 35,000 (Jewitt and Luu, 1995). If recent Hubble Space Telescope observations are correct, the number of km sized and larger bodies may approach 1 billion.

The Kuiper Belt is the suspected source of the Jupiter-family short-period comets (SPCs). These small, ice-rich bodies have dynamical and physical lifetimes that are short compared to the age of the Solar System. If a steady state population is to be maintained, the comets in the inner Solar System must be resupplied from a longer-lived source elsewhere. While it has long been thought that SPCs are captured from long-period orbits by the action of the gas giant planets (especially Jupiter), this explanation has recently been shown to be invalid. In particular, the highly anisotropic distribution of orbital inclinations of the Jupiter-family SPCs argues for a flattened (disk-shaped) source, exactly as is observed among the Kuiper Belt objects (Duncan et al., 1988). Therefore, in the presently accepted view, the long-period comets are eroded from the Oort Cloud by external gravitational perturbations, while the SPCs have a separate and distinct source in the trans-Neptunian region. A mission to the Kuiper Belt therefore is a mission to the birth site of the comets.

The Kuiper Belt is likely a remnant of the much more extensive (and long gone) protoplanetary disk of gas and dust from which the solid objects of the Solar System formed, a conclusion that has been strengthened by very recent dynamical simulations (Duncan et al., 1995).

With the density of 100-km diameter Kuiper Belt objects being of order 1 per AU^3, the characteristic separation of these bodies is of order 1 AU. This means that, without any extra efforts on the part of Pluto Express, the post-Pluto encounter trajectory would pass (on average) about 1/2 AU from one or more large Kuiper Belt Objects. This is a pessimistic estimate of the distance of closest approach for two reasons. First, there will be many opportunities (roughly one for each year of flight) for close encounters along the spacecraft trajectory in the years following the Pluto flyby. It is likely that several of them will occur at distances considerably smaller than 1 AU from the spacecraft. Second, and more importantly, Pluto Express will contain propellant sufficient to permit the spacecraft to be steered towards known Kuiper Belt objects. Accordingly, one or more post-Pluto encounters with objects in the Kuiper Belt almost certainly will be possible (encounters prior to arrival at Pluto are ruled out by the tight requirements imposed on the Pluto encounter geometry).

10. Origin of the Pluto-Charon Binary

The origin of the Pluto-Charon binary itself was recognized as a significant problem almost as soon as Charon was discovered by Christy and Harrington (1978). The noteworthy aspects of the binary are: (i) the small, 2:1 size ratio noted above; (ii) the complete tidal evolution of the system exhibited in the spin:spin:orbit synchronicity of Pluto's rotation period, Charon's rotation period, and Charon's orbital period; (iii) the high specific angular momentum of the system, which is close to the stability threshold for a spinning body; and (iv) the dissimilarity of Pluto and Charon with regard to their surface appearances, compositions, and perhaps their bulk densities.

These constraints have been considered by various workers, including McKinnon (1984; 1989), Peale (1986), Simonelli et al. (1989), Stern (1991), and Levison and Stern (1995). The specific angular momentum of the system does not permit either a fission or co-accretion origin. The only origin scenario for the binary that appears to satisfy all of the available constraints (as for the Earth-Moon system) is characterized by a "giant" collision between Pluto and some object several hundred to perhaps 1000 km in diameter. According to this formation scenario for the binary, the collision spilled enough material from Pluto and into orbit around it to generate Charon. Once Charon formed, it tidally evolved to its present orbit in $> 10^7$ years. Charon's surface color, albedo, and composition are believed to result from the much more effective role of atmospheric escape on Charon (Trafton et al. 1988), which led to a rapid loss of volatiles and the subsequent darkening of the remaining, H_2O-ice lag deposits (cf., also Johnson 1989; Stern 1990). Charon's surface properties may also in part be related to its possibly different internal volatile fraction, which itself may be related to the impact parameter and energetics of the giant collision.

An important qualitative difference between the Pluto-Charon and Earth-Moon giant-impacts is that the relative collision velocities, and hence impact energies of the Pluto-Charon event, were much smaller. This enormously ameliorated the resultant thermal effects at Pluto (McKinnon 1989). Thus, whereas the Earth may have been left molten by the Mars-sized impactor necessary to have created the Moon, the proto-Charon impactor would probably only raise Pluto's global mean temperature by no more than 50-75 K. This is insufficient to melt either body, but may have been sufficient to trigger internal differentiation. It would have also produced a substantial transient, post-impact, hot, volatile atmosphere with intrinsically high escape rates, fractionating Pluto's present-day volatile content (cf. McKinnon 1989; Lunine and Nolan, 1992).

If Pluto and some proto-Charon impactor did form in heliocentric orbit, why should these two objects, alone in over 10^3 AU^3 of space, "find" each other in order to execute a mutual collision? That is, the impact hypothesis fails to explain the fact that the collision producing the impact was highly unlikely, if Pluto and proto-Charon were the only large bodies in the 30-50 AU region. McKinnon (1984) was the first to discuss this point. Later, Stern (1991) pointed out that this issue, as well as the capture of Triton from heliocentric orbit and the tipping of the obliquities of Uranus and Neptune, could all be rationalized if Pluto and proto-Charon were members of a large, ancient population of some > 300-3000 small ($10^{24.5-25.5}$ gm) precursor objects present during the accretion of Uranus and Neptune. As shown through statistical arguments in that paper, the presence of 300-3000 1000-km diameter and larger objects in the Uranus-Neptune zone makes the Uranus/Neptune tilting, Triton's capture, and the formation of the Pluto-Charon binary each likely. Stern (1991) also showed that the vast majority of these ice dwarfs were scattered (with the comets) to the Oort Cloud and Kuiper Belt by strong perturbations from Neptune and Uranus. Pluto-Charon and Triton remain in the 20-30 AU zone today only because they are trapped in unique dynamical niches that protect them against loss to strong perturbations. This hypothesis implies that Pluto and Triton are important "relics" of a very large population of icy bodies, which by number (but not by mass) dominate the planetary population of the Solar System. As such, these interesting bodies no longer appear to be isolated anomalies in the architecture of the outer Solar System but are instead seen to be genetic relations from a heterogeneous ensemble of precursor objects that were previously not recognized as a large class unto themselves.

11. Implications for the Formation of the Solar System

The Pluto/Charon system lies on the inner edge of the Kuiper Belt, and in consequence represents the largest and best-studied example of solid material out of which the giant planets were formed. It has become increasingly likely, based on astronomical studies of other disks in star-forming regions as well as spacecraft and Earth-based study of our own Solar System, that proto-planetary disks are both pervasive and chemically complex (Figure 6).

Pluto and Charon reside in a region of the Solar System corresponding to that part of the protoplanetary disk in which infalling primitive grains were only partially heated and altered, and where nebular gas likely retained a strong signature of interstellar composition. These assertions are exciting in that they argue for a strong link with the original, nascent molecular cloud.

The important dynamical relationship established between Kuiper Belt objects, short period comets and Pluto/Charon enables the possibility of studying material over a range of sizes from a common region of the protoplanetary disk. Size is an important indicator of the amount of post-formation processing of material. Interestingly, although Pluto may be evolved relative to the smaller Kuiper Belt and cometary objects, its size has also

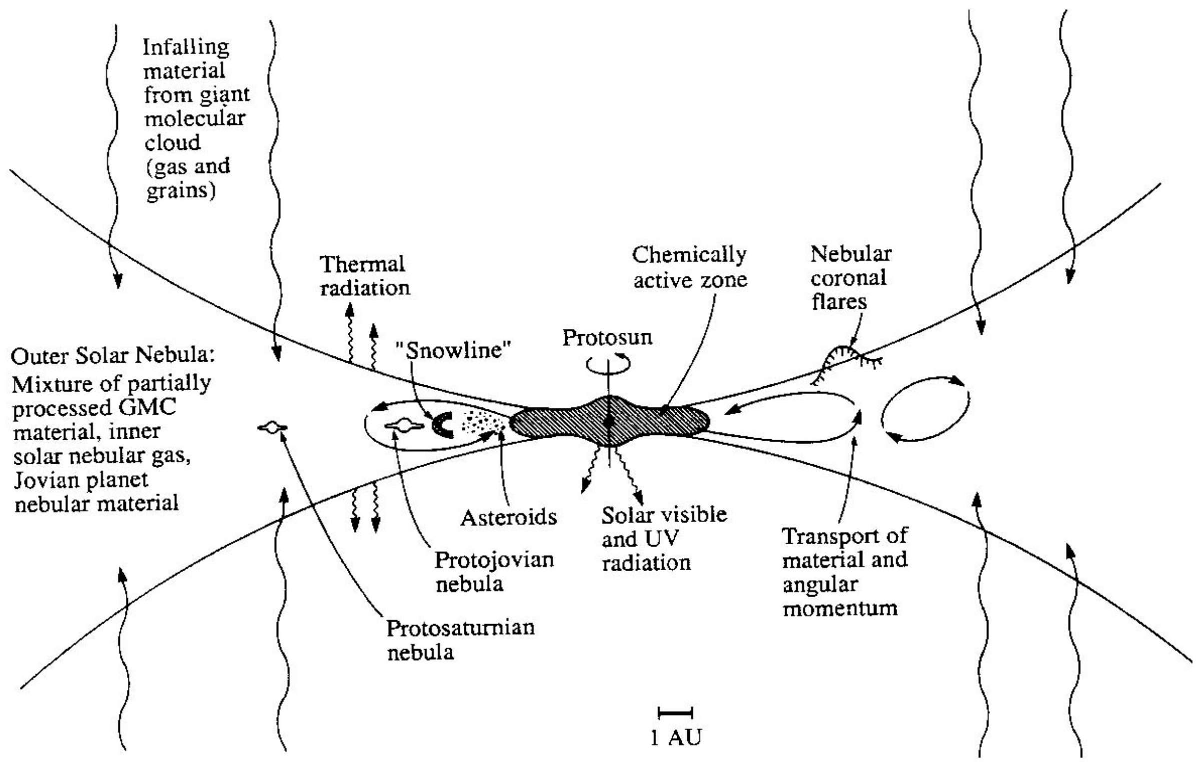

Figure 6: Schematic of selected physical and chemical processes in the precursor of our Solar System, the so-called *solar nebula*. From Lunine 1989.

allowed volatiles from its interior to be outgassed to the surface, where they are accessible to observation. We do not know whether smaller Kuiper Belt objects have exposed volatiles.

Detailed study of the full range of objects from Pluto down through short period comets will constrain the composition and history of this material, which represents primitive icy material in much the same way that the carbonaceous chondrites are samples of primitive rocky and refractory-organic material. In particular, it may be possible to constrain the amount of radial mixing of solid and gaseous volatiles from the outer to inner solar nebula by detailed analysis of such material (Lunine et al., 1991; 1995). This, in turn, represents a primary chemical constraint on mechanisms of angular momentum and energy transport through the nebula, a key issue in understanding how proto-planetary disks work (Cassen, 1995). Relating the composition of the ices on Pluto, the Kuiper Belt and short-period cometary bodies to measurements in the Jovian atmosphere and Titan's atmosphere by *Cassini* and *Galileo* will allow construction of a history of the volatile molecular species from infall into the disk through the early history of planet formation.

12. References:

1. Albrecht, R., C. Barbieri, H.-M. Adorf, G. Corrain, A. Gemmo, P. Greenfield, O. Hainaut, R. N. Hook, D. J. Tholen, J. C. Blades, and W. B. Sparks 1994. High-resolution imaging of the Pluto-Charon system with the Faint Object Camera of the Hubble Space Telescope. *Astrophys. J. Lett*., 435, L75-L78.
2. Bagenal., F., and R.L. McNutt, 1989. Pluto's interaction with the solar wind. *Geophys. Res. Lett*. 16, 1229-1232.
3. Belcher, J.W., A.J. Lazarus, R.L. McNutt, G.S. Gordon. 1993. Solar wind conditions in the outer heliosphere and the distance to the terminal shock, *J. Geophys*. *Res*. 98, 15177-15183.
4. Buie, M.W., D.P. Cruikshank, L.A. Lebofsky, E.F. Tedesco, 1987. Water frost on Charon. *Nature,* 329, 522-523.
5. Buie, M. W., and D. J. Tholen 1989. The surface albedo distribution of Pluto. *Icarus,* 79, 23-37.
6. Buie, M. W., D. J. Tholen, and K. Horne 1992. Albedo maps of Pluto and Charon: Initial mutual event results. *Icarus,* 97, 211-227.
7. Buie, M. W., D. J. Tholen, and L. H. Wasserman 1997. Separate lightcurves of Pluto and Charon. *Icarus*, 125, 233-244.
8. Cassen, P. 1995. Utilitarian models of the solar nebula. *Icarus*, 112, 405-429.
9. Chamberlain, J.W. and D.M. Hunten 1987. *Theory of Planetary Atmospheres*, Academic Press, New York.
10. Christy, J.W. and R.J. Harrington, 1978, "The Satellite of Pluto," *Astron. J.* 83, 1005-1008.
11. Duncan, M., T. Quinn and S. Tremaine 1988. The origin of short-period comets. *Astrophys. J. Lett*., 328, 69-73.
12. Duncan, M.J., H.F. Levison and S.M. Budd. 1995. The dynamical structure of the Kuiper belt. *Astron. J*., 110, 3073-3081.
13. Elliot, J. L., E. W. Dunham, A. S. Bosh, S. M. Slivan, L. A. Young, L. H. Wasserman, and R. L. Millis 1989. Pluto's atmosphere, *Icarus*, 77, 148.
14. Elliot, J. L., and L. A. Young 1991. Limits on the radius and a possible atmosphere of Charon from its 1980 stellar occultation. *Icarus*, 89, 244-254.
15. Eshleman, V.R. 1989. Pluto's atmosphere: models based on refraction, inversion and vapor-pressure equilibrium. *Icarus*, 80, 439-443.
16. Galeev, A. A., T. E. Cravens, and T. I. Gombosi 1985. Solar wind stagnation near comets, *Astrophys. J*. 289, 807-819.

17. Goldreich, P., N. Murray, P.Y. Longaretti, and D. Banfield. 1990. Neptune's story. *Science*, 245, 500-504.

18. Hansen, C.J., A.S. McEwen, A.P. Ingersoll, and R.J. Terrile 1990. Surface and airborne evidence for plumes and winds on Triton, *Science*, 250, 421-424.

19. Hansen, C. and D. A. Paige, 1996. Seasonal Nitrogen Cycles on Pluto. *Icarus*, 120, 247-265.

20. Hubbard, W. B., D.M. Hunten, S.W. Dieters, K.M. Hill, and R.D. Watson 1988. Occultation evidence for an atmosphere on Pluto, *Nature*, 336, 452.

21. Hubbard, W. B., R. V. Yelle, J. I. Lunine, 1990. Nonisothermal Pluto atmosphere models. *Icarus*, 84 1-11.

22. Hunten, D.M. and A.J. Watson. 1982. Stability of Pluto Atmosphere. *Icarus*, 665-67.

23. Ingersoll, A.P. 1990. Dynamics of Triton's atmosphere. *Nature*, 344 315-317.

24. Ip, W.-H. 1990. On the ionosphere of Triton: An evaluation of the magnetospheric electron precipitation and photoionization effects, *Geophys. Res. Lett*., 17, 1713-1716.

25. Jewitt, D.C. 1994. Heat from Pluto. *Astron. J*., 107, 372-378.

26. Jewitt, D.C. and J.X. Luu 1993. Discovery of the candidate Kuiper Belt object 1992QB1. *Nature*, 362, 730-732.

27. Jewitt, D.C. and J.X. Luu 1995. The Solar System beyond Neptune. *Astron. J.*, 109, 1867-1876.

28. Johnson, R. E. 1989. Effect of irradiation on the surface of Pluto, *Geophys. Res. Lett.*, 16, 1233-1236.

29. Kecskemety, K., and T. E. Cravens, 1993. Pick-up ions at Pluto, *Geophys. Res. Lett*, 20, 543.

30. Kivelson, M.G., L.F. Bargatze, K.K. Khurana, D.J. Southwood, R.J. Walker, and P.J. Coleman 1993. Magnetic signatures near Galileo's closest approach to Gaspra, *Science*, 261, 331-334.

31. Lanzerotti, L. J., W. L. Brown, C. G. Maclennan, A. F. Cheng, S. M. Krimigis, and R. E. Johnson 1987. Effects of charged particles on the surfaces of the satellites of Uranus, *J. Geophys. Res.*, 92, 14949-14957.

32. Lellouch, E. 1994. The thermal structure of Pluto's atmosphere: clear vs. hazy models. *Icarus,* 108. 255-264.

33. Levinson, H. and S.A. Stern 1995. Possible origin and early evolution of the Pluto-Charon Binary. *Icarus*, 116, 315-339.

34. Luhmann, J. G., 1986. The solar wind interaction with Venus, *Space Sci. Rev*., 44, 241.

35. Lunine, J.I. 1989. The Urey Prize lecture. Volatile processes in the outer Solar System. *Icarus*, 81, 1-13.

36. Lunine, J.I., S. Engel, B. Rizk, and M. Horanyi 1991. Sublimation and reformation of icy grains in the primitive solar nebula. *Icarus*, 94, 333-343.

37. Lunine, J.I. and M.C. Nolan 1992. A massive early atmosphere on Triton. *Icarus*, 100, 221-234.

38. Lunine, J.I., W. Dai, and F. Ebrahim 1995. Solar system formation and the distribution of volatile species. in *Proc. Conf. Deep Earth and Planetary Volatiles* (K. Farley, ed.). AIP Press, New York, pp. 117-122.

39. Majeed, T., J. C. McConnell, D. F. Strobel, and M. E. Summers. 1990. The ionosphere of Triton, *Geophys. Res. Lett*., 17, 1721-1724.

40. Marcialis, R. L. 1983. A two-spot model for the surface of Pluto. *Master's thesis*, Vanderbilt University.

41. Marcialis, R.L., G.H. Rieke, L.A. Lebofsky, 1987. The surface composition of Charon: Tentative identification of water ice. *Science,* 237, 1349-1351.

42. McKinnon, W.B., 1984. On the origin of Pluto and Triton. *Nature*, 311, 355-358.

43. McKinnon, W.B., 1989. On the origin of the Pluto-Charon binary. *Ap. J. Lett*., 344, L41-44.

44. McKinnon, W.B. and S. Mueller, 1988. Pluto's structure and composition suggest origin in the solar, not a planetary nebula. *Nature*, 335, 240-242.

45. McKinnon, W.B., G, Schubert and D. Simonelli 1997. Interior structures and thermal evolution of Pluto and Charon. In *Pluto and Charon* (eds. S.A. Stern and D. J. Tholen) U of Arizona Press, Tucson.

46. McNutt, R. L., Jr., and J. D. Richardson, 1988, Constraints on Titan's ionosphere. *Geophys. Res. Lett.*, 15, 709-712.

47. McNutt, R.L., Jr. 1989. Models of Pluto's upper atmosphere, *Geophys. Res. Lett*., 16, 1225-1228.

48. Mendis, D.A., E.J. Smith, B.T. Tsurutani, J.A. Slavin, D.E. Jones and G.L. Siscoe. 1986. Comet-solar wind interaction: Dynamical length scales and models, *Geophys. Res. Lett*., 13, 239.

49. Millis, R. L., L. H. Wasserman, O. G. Franz, R. A. Nye, J. L. Elliot, E. W. Dunham, A. S. Bosh, L. A. Young, S. M. Slivan, A. C. Gilmore, P. M. Kilmartin, W. H. Allan, R. D. Watson, S. W. Dieters, K. M. Hill, A. B. Giles, G. Blow, J. Priestly, W. M. Kissling, W. S. G. Walker, B. F. Marino, D. G. Dix, A. A. Page, J. E. Ross, H. P. Avey, D. Hickey, H. D. Kennedy, K. A. Mottram, G. Moyland, T. Murphy, C. C. Dahn, and A. R. Klemola 1993. Pluto's radius and atmosphere: Results from the entire 9 June 1988 occultation data set. *Icarus*, 105, 282-297.

50. Neubauer, F.M., A. Luttgen, and N.F. Ness. 1991. On the lack of a magnetic signature of Triton's magnetospheric interaction on the Voyager 2 flyby trajectory, *J. Geophys. Res., Suppl*., 96, 19,171-19,175.

51. Neugebauer, M. 1990. Spacecraft observations of the interaction of active comets with the solar wind, *Rev. Geophys*. 28, 231-252.

52. Null, G.W., W.M. Owen, and S.P. Synott, 1993. Masses and Densities of Pluto and Charon. *Astron*. *J*., 105, 2319-2335.

53. Owen, T.C., T.L. Roush, D.P. Cruikshank, J.L. Elliot, L.A. Young, C. DeBergh, B. Schmitt, T.R. Geballe, R.H. Brown, and M.J. Bartholomew, 1993. Surface ices and the atmospheric composition of Pluto. *Science*, 261, 745-748.

54. Peale, S.J. 1986, "Orbital Resonances, Unusual Configurations and Exotic Rotation States Among Planetary Satellites," in *Satellites* (eds. J.A. Burns and M.S. Matthews), University of Arizona Press, Tuscon.

55. Reinsch, K., V. Burwitz, M.C. Festou. 1994. Albedo Maps of Pluto and Improved Physical Parameters of the Pluto Charon System. *Icarus*, 108, 209-218.

56. Roush, T. 1994. Charon: more than water ice? *Icarus*, 108, 243-254.

57. Russell, C.T., D.N. Baker and J.A. Slavin, 1988, The magnetosphere of Mercury, in *Mercury*, Vilas, Chapman and Mathews, eds., U. of Arizona Press, 1988.

58. Simonelli, D.P. and R.T. Reynolds, 1989. The interiors of Pluto and Charon: Structure, composition, and implications. *Geophys. Res. Lett.*, 16, 1209-1212

59. Spencer, J.R., L.M. Trafton, J.A. Stansberry, E.F. Young, R.P. Binzel, and S.K. Croft 1997. Volatile transport, seasonal cycles, and atmospheric dynamics on Pluto, in *Pluto and Charon* (eds. S.A. Stern and D.J. Tholen), Univ. of Arizona Press, Tucson, 1997.

60. Stansberry, J. A., J. I. Lunine, W. B. Hubbard, R. V. Yelle, and D. M. Hunten, 1994. Mirages and the nature of Pluto's atmosphere, *Icarus*, 111, 501-513.

61. Stansberry, J.A., J.R. Spencer, B. Schmitt, A. Becnhkoura, R.V. Yelle and J.I. Lunine, 1996. A model for the overabundance of methane in Pluto's atmosphere. *Planetary and Space Science*, 44, 1051-1063.

62. Stern, S.A. 1988. Constraints on Pluto's density and composition. *Icarus*, 74, 269-278

63. Stern, 1990, "Rotationally resolved UV spectra of Pluto and Triton from 2600-3150Å", *Bul. Am. Astron*. *Soc*., Vol. 22, No. 3, p.1130.

64. Stern, S.A., 1991. On the Number of Planets in the Solar System: Evidence of a Substantial Population of 1000-km Bodies. *Icarus*, 90, 271-281

65. Stern, S.A., 1992. The Pluto-Charon system. *Ann. Revs. Astron. Astrophys.,* 30, 185-233.

66. Stern, S.A., and D.J. Tholen (eds.), *Pluto and Charon,* University of Arizona Press, 1997.

67. Stern, S.A., D.A. Weintraub and M.C. Festou 1993. *Science*, 261, 1713-1716.

68. Stern, S.A., M.W. Buie, and L.M. Trafton, 1997, *The Astronomical Journal*, Vol 113, 827.

69. Strobel, D. F., A. F. Cheng, M. E. Summers, and D. J. Strickland. 1990. Magnetospheric interaction with Triton's ionosphere, *Geophys. Res. Lett*., 17, 1661-1664.

70. Strobel, D., X. Zhu, M.E. Summers and M.H. Stevens. 1996. On the vertical thermal structure of Pluto's atmosphere. *Icarus*, 120, 266-289.

71. Summers, M. and D.F. Strobel. 1997. Chemical models of Pluto's atmosphere. In *Pluto and Charon*, eds. S.A. Stern and D. Tholen. Tucson, U. Ariz. Press.

72. Sykes, M.V., R.M. Cutri, L.A. Lebofsky, and R.P. Binzel. 1987. IRAS serendipitous survey observations of Pluto and Charon. *Science*, 237, 1336-1339.

73. Tholen, D. J., and M. W. Buie 1997. The orbit of Charon. I. New Hubble Space Telescope observations. *Icarus*, 125, 245-260..

74. Thompson, W. R., B. G. J. P. T. Murray, B. N. Khare, and C. Sagan. 1987. Coloration and darkening of methane clathrate and other ices by charged particle irradiation: Application to the outer Solar System, *J. Geophys. Res.,* 92, 14933-14947.

75. Trafton, L. 1980. Does Pluto have a substantial atmosphere? *Icarus*, 44, 53-61..

76. Trafton, L.M., and S.A. Stern, 1983. The global distribution of Pluto's atmosphere. *Ap. J.*, 267, 872-881.

77. Trafton, L.M., S.A. Stern, G.R. Gladstone. 1988. The Pluto Charon System-The Escape of Charon Primordial Atmosphere. *Icarus*, 74, 108-120.

78. Tryka, K., R.H. Brown, D.P. Cruikshank, T.C. Owen, T.R. Geballe and C. deBergh 1994. Temperature of nitrogen ice on Pluto and its implications for flux measurements, *Icarus*, 112, 513-527.

79. Tyler, G. L., et al. 1989. Voyager radio science observations of Neptune and Triton, *Science*, 246, 1466-1473.

80. Yelle, R. V., and J. I. Lunine 1989. Evidence for a molecule heavier than methane in the atmosphere of Pluto. *Nature*, 339, 288-290.

81. Yelle, R.V. et al. 1995. in *Neptune and Triton* (ed. D.P. Cruikshank), Univ. of Arizona Press, Tucson.

82. Yelle, R.V. and J. Elliot 1997. in *Pluto and Charon* (eds. S.A. Stern and D. J. Tholen). Univ. of Arizona Press, Tucson.

83. Young, E. F., and R. P. Binzel 1993. Comparative mapping of Pluto's sub-Charon hemisphere: Three least squares models based on mutual event lightcurves. *Icarus* 102, 134-149.

84. Young, L.A. 1994. *Bulk Properties and Atmospheric Structure of Pluto and Charon*, Dissertation, MIT.

85. Young, L. A., C. B. Olkin, J. L. Elliot, D. J. Tholen, and M. W. Buie 1994. The Charon-Pluto mass ratio from MKO astrometry. *Icarus* 108, 186-199.